REGULAR PAPER

DOI: 10.1007/s40684-018-0063-0
ISSN 2288-6206 (Print) / 2198-0810 (Online)

Diffusion Enhancement during Electrically Assisted Brazing of Ferritic Stainless Steel Alloys

Viet Tien Luu[1], Thi Kieu Anh Dinh[1], Hrishikesh Das[1], Ju-Ri Kim[1], Sung-Tae Hong[1,#], Hyun-Min Sung[2], and Heung Nam Han[2,#]

1 School of Mechanical Engineering, University of Ulsan, 93, Daehak-ro, Nam-gu, Ulsan, 44610, Republic of Korea
2 Department of Materials Science & Engineering and Center for Iron & Steel Research, RIAM, Seoul National University, 1, Gwanak-ro, Gwanak-gu, 08826, Republic of Korea
Corresponding Author / E-mail: sthong@ulsan.ac.kr, TEL: +82-52-259-2129
E-mail: hnhan@snu.ac.kr, TEL: +82-2-880-9240
ORCID: 0000-0003-2263-7099

KEYWORDS: Electrically assisted, Brazing, Diffusion, Stainless steels

The electrically assisted brazing of a ferritic stainless steel with nickel-based filler metal is experimentally investigated. During electrically assisted brazing of a lap joint, the temperature of the joint is first rapidly increased to a brazing temperature and held nearly constant for a specific period using a pulsed electric current. Microstructural analysis results strongly suggest that the electric current during electrically assisted brazing enhances diffusion between the filler metal and the ferritic stainless steel, thus inducing significantly thicker diffusion zones compared with induction brazing. The mechanical test results show that the strength of the electrically assisted brazing joint is comparable to or even superior to those of the joint fabricated by induction brazing, while the process time of the electrically assisted brazing is significantly shorter than that of induction brazing.

Manuscript received: July 28, 2017 / Revised: October 23, 2017 / Accepted: January 11, 2018

1. Introduction

Ferritic stainless steels are widely used in automotive industries, especially for exhaust systems including manifolds, catalytic converters, mufflers, and tail pipes. Ferritic stainless steels are well known for their excellent stress corrosion cracking resistance, adequate high temperature resistance to oxidation, good weldability, and good forming characteristics.[1,2] However, the heat generated during conventional fusion welding processes of these stainless steels may lead to grain coarsening in the welded region, since they directly solidify from a liquid phase to the ferrite phase without any intermediate phase transformation.[3,4] Grain coarsening in the welded region may reduce the toughness, ductility, and corrosion resistance of the joint. Also, conventional fusion welding processes may not be suitable for joining thin stainless steel sheets and may make it difficult to accommodate the recent industrial trends of using thinner sheet materials for weight reduction.

Brazing is a metal-joining process in which work pieces are joined by melting and solidifying a filler material without melting the work pieces. Since brazing does not require melting the work pieces, very thin metal sheets that are less than a millimeter in thickness can be easily joined by brazing. The brazing of stainless steel sheets has been frequently studied.[5-8] Shiue et al.[5] studied the infrared brazing of 403 martensitic stainless steel with a nickel (Ni)-based braze alloy, and they achieved a joint strength close to 300 MPa with brittle failure. Ou et al.[6] studied infrared brazing of 422 stainless steel using a BNi-2 braze alloy as a filler metal; they observed a decrease in the shear strength of the brazed joint with increasing brazing temperature and/or time. Wu et al.[7] investigated induction brazing of Inconel X-750 to stainless steel 304 and reported that the width of the braze-affected zone increased with increasing joining time. Lugscheider et al.[8] studied the brazing of 316 stainless steel with BNi-2, BNi-5 and BNi-7 filler metals to determine the effects of brazing temperature, time, post-braze heat treatment, and brazing clearance on the metallurgical quality and tensile strength of the joints. They reported that the 316 stainless steel braze joint with BNi-5 filler metal showed the maximum joint strength.

While various heat sources are available for successful brazing of stainless steels as mentioned above, the resistance heating can also be a very effective heat source for brazing. The effectiveness of resistance heating as a heat source for brazing may be accompanied by the benefits of rapid heating and the possibility of additional athermal effects associated with the electric current. Specifically, the electric

current may induce the electroplasticity, wherein the electric current enhances the mobility of atoms in addition to the well-known effect of elevated temperature by resistance heating.[9-15] While a clear explanation of the atomic-level mechanism of electroplasticity is still being discussed, attempts to utilize the thermal/athermal effects of electric current in various manufacturing processes (electrically assisted manufacturing, EAM) have been reported.[13] For example, Xu et al.[16] suggested an electrically assisted solid-state pressure welding process of 316 stainless steel and reported that the maximum shear strength was achieved with increased current density. Kim et al.[17] studied electrically assisted blanking, which exploits the electroplasticity of ultra-high strength steel. Their experimental results showed that the blanking load of electrically assisted blanking was clearly lower than that of blanking immediately after local resistance heating. Baranov et al.[18] suggested an electroplastic metal cutting process and reported that the friction force and processing time were significantly reduced by applying a pulsed electric current. It also needs to be mentioned that under certain process conditions, the results for some selected EAMs have been described without considering the athermal effects of electric current. For example, Ng et al.[19] suggested using electric current in the roll bonding process and used the joule heating effect to explain the result that electrically assisted roll bonding lowered rolling forces and increased the joint strength of bonded sheets.

In the present study, we explored the unique features of electrically assisted brazing of ferritic stainless steels using a nickel-based filler metal. In electrically assisted brazing, only the filler metal melts and solidifies, unlike conventional resistance spot welding. The microstructural and mechanical properties of the electrically assisted brazing joints were experimentally compared with those of induction brazing. Athermal effects of the electric current in electrically assisted brazing are discussed based on the experimental results.

2. Experimental Set-Up

In the present study, 436 ferritic stainless steel sheets with a thickness of 0.8 mm were used for the experiments. The chemical composition of the 436 ferritic stainless steel is listed in Table 1. Brazing specimens with a length of 100 mm and a width of 20 mm were fabricated from the ferritic stainless steel sheet by laser cutting along the rolling direction of the sheet. A nickel (Ni)-based filler metal (AMS 4777, Lucas-Milhaupt Incorporated, USA) film with a thickness of 76 μm was used for brazing, and its chemical composition is also listed in Table 1. The Ni-based filler metal film was cut to sizes of 20 mm × 20 mm and was placed at the interface of the two brazing specimens, while the overlap length of the two brazing specimens was fixed at 40 mm, as schematically shown in Fig. 1(a). Two different heating methods, resistance heating (electrically assisted brazing) and induction heating (induction brazing), were used to fabricate lap joints via brazing. Note that the induced eddy current during induction heating is a surface phenomenon (or simply a skin effect).[20] The thermal homogeneity during induction heating is mostly obtained by thermal conduction.

For electrically assisted brazing with resistance heating, a programmable welder (VADAL SP-1000U, Hyosung, South Korea) was used to apply an electric current to the specimens. A pair of copper electrodes was used to clamp the brazing specimens, and an electric current was applied through the joint of the specimens, as described in Fig. 1(b). A custom made 25 kW induction brazing machine (SK brazing Corporation, South Korea) with a maximum frequency of 440 kHz was used for induction brazing. The assembly of brazing specimens with the Ni-based filler (Fig. 1(a)) was placed inside an induction coil, as described in Fig. 1(c).

A pulsed electric current was used for electrically assisted brazing. During electrically assisted brazing, the temperature of the assembly of brazing specimens with Ni-based filler (simply, the joint temperature) was rapidly increased to the brazing temperature (≈1100°C) using the electric current, which had a magnitude of I_i and a duration of t_i. The joint temperature was then held nearly constant for an additional holding time t_h by periodically applying an electric current I_m with a duration of t_m and a period of μ_m, as schematically described in Fig. 2(a). During induction brazing, the joint temperature also increased to the target value (≈1100°C) and was then held nearly constant for a holding time t_h by the induction coil, as schematically described in Fig. 2(b). The heating parameters for the electrically assisted brazing and the induction brazing are listed in Table 2. Note that for the zero holding time (t_h = 0 sec), the joint was simply cooled down to room temperature immediately after the joint temperature reached the target brazing temperature. During electrically assisted and induction brazing, the temperature history of the joint was measured using an infrared thermal imaging camera (T621, FLIR, Sweden), which was calibrated in separate preliminary experiments with a k-type thermocouple, and a k-type thermocouple, respectively.

After brazing, the cross-sectional samples were prepared along the width direction at the center of the joint for microstructural analysis. The cross-sectional samples were processed using a standard metallographic grinding and polishing procedure, and were finished with a 1 μm diamond suspension followed by electrical polishing with colloidal silica. The cross-sectional samples were first examined using a scanning electron microscope (SEM) to confirm that the brazing joint was successfully fabricated without any macroscopic defects with the heating parameters in Table 2. The microstructure was then observed using a field emission scanning electron microscope (FE-SEM: SU70, Hitachi, Japan) equipped with an electron backscatter diffraction system (EBSD: EDAX-TSL Hikari, USA) and an energy dispersive spectrometer (EDS: X-Max50, Horiba, Japan). Finally, the mechanical properties of the joint were evaluated by simple tensile lap-shear tests using a universal testing machine with a constant displacement rate of 2 mm/min.

3. Results and Discussion

The temperature histories during electrically assisted brazing show that the joint temperature rapidly reached the brazing temperature (≈1100°C) and was held nearly constant during the remaining process time (Fig. 3(a)). The temperature histories of the induction brazing are shown in Fig. 3(b). Note that the time to reach the target brazing temperature was much longer for the induction brazing (approximately 15 sec) than for the electrically assisted brazing (1.1 sec). Therefore, for

Table 1 Chemical composition of ferritic stainless steel and filler material (AMS 4777)

Materials	Chemical composition (wt%)										
	Fe	Cr	Si	B	Ni	N	P	C	S	Mo	Mn
436 Ferritic stainless steel	Bal.	17.0-20.0	1.00	-	0.6	0.025	0.04	0.025	0.03	0.4-0.8	1
AMS 4777	3.0	7.0	4.5	3.1	Bal.	-	-	-	-	-	-

Table 2 Heating parameters for electrically assisted brazing and induction brazing

Type	Electric current I_i (A)	Duration time t_i (sec)	Electric current I_m (A)	Period time μ_m (sec)	Duration time t_m (sec)
Electrically assisted brazing	2500	1.10	750	0.5	0.5
Induction brazing	Induction power (%)		Heating time (sec)		Holding time (sec)
	75		15		0, 10, 20

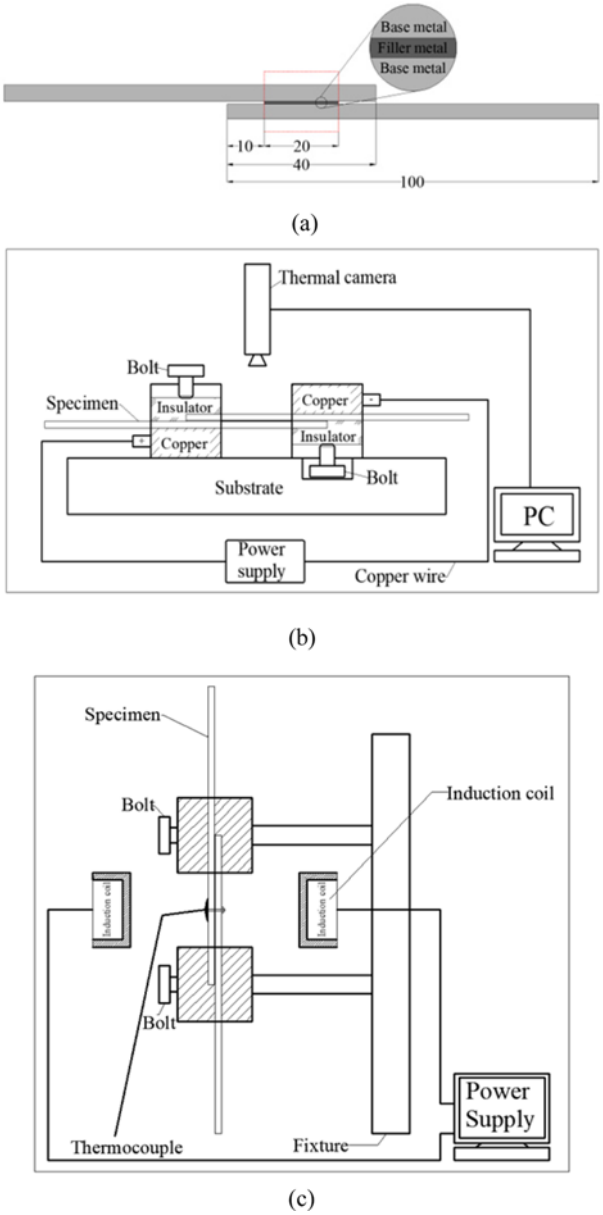

Fig. 1 (a) Schematic of brazing specimen and the experimental set-up for: (b) electrically assisted brazing and (c) induction brazing

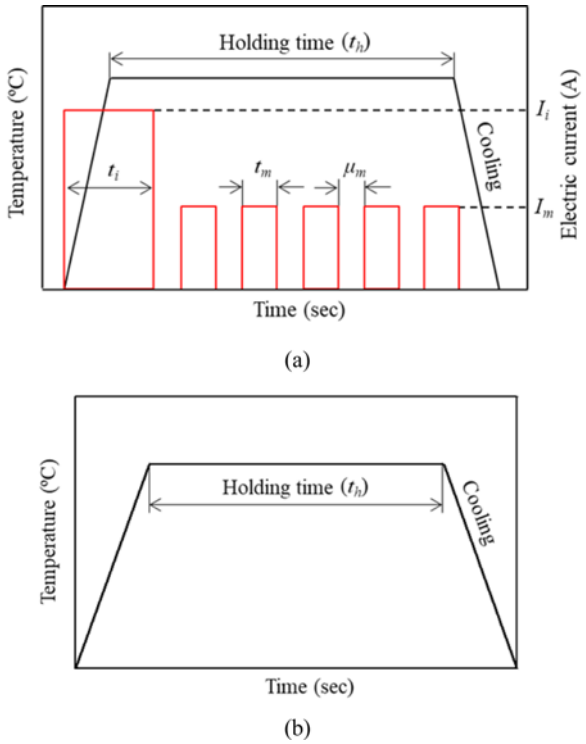

Fig. 2 Schematic of temperature histories for (a) electrically assisted brazing and (b) induction brazing

the same holding time t_h a higher amount of thermal energy was provided to the joint in induction brazing than in electrically assisted brazing even though the effect may not be significant, since the intensity of diffusion at temperatures below the liquidus of the filler metal would be relatively low.

For both electrically assisted brazing and induction brazing, the 436 ferritic stainless steel specimens were successfully joined using the Ni-based filler metal without any visible porosity or macroscopic defects, even for $t_h = 0$ sec, as shown in the SEM images of the cross-sections of the joints (Fig. 4(a)). As marked in Figs. 4(a) and 4(b), it was observed that all the brazing joints consist of three distinctively different zones, i.e., the base metals, the diffusion zone, and the interlayer (or the filler metal). The SEM images of the interlayer show bright and dark phases for all the electrically assisted and induction brazing joints (Fig. 4(c)). The results of EDS point scan analysis on the bright and dark phases in the interlayer reveal that the bright phase is primarily composed of Ni (~44 wt%) and Fe (~40 wt%) with different alloying element concentrations, while the dark phase is composed of

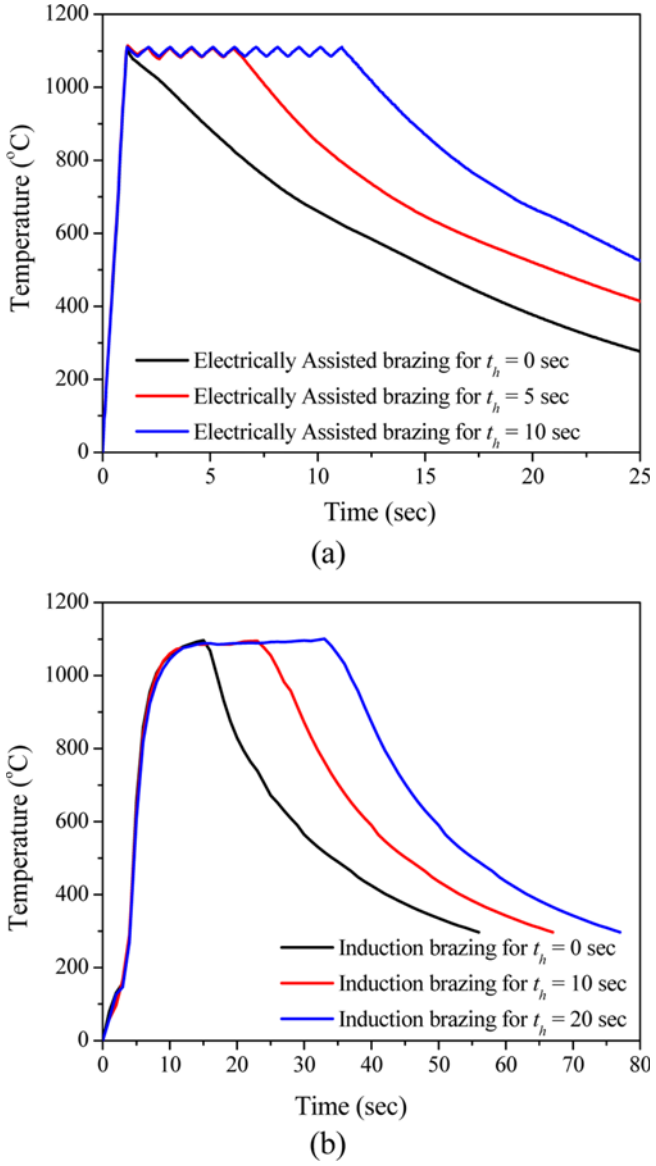

Fig. 3 Temperature histories of (a) electrically assisted brazing and (b) induction brazing for various brazing conditions

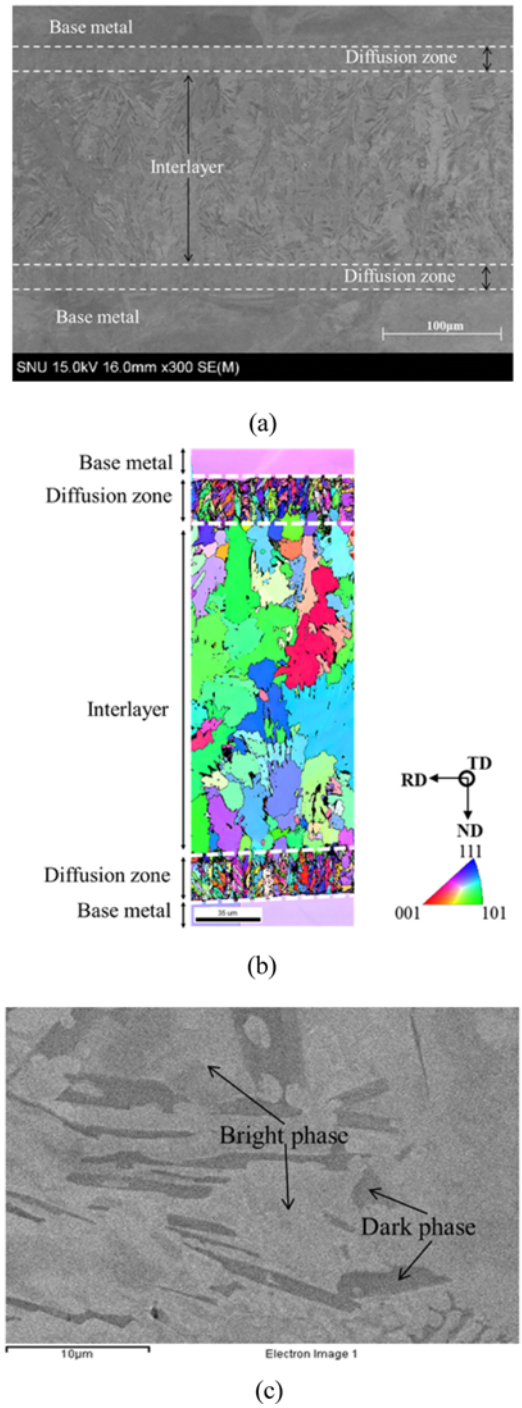

Fig. 4 Cross-sectional images: (a) SEM micrograph of electrically assisted brazing (t_h = 0 sec), (b) EBSD inverse pole (IPF) map of electrically assisted brazing (t_h = 5 sec), and (c) SEM micrograph of interlayer (filler metal) of electrically assisted brazing (t_h = 0 sec)

B (~15 wt%), Cr (~37 wt%), Fe (~36 wt%), and a smaller amount of Ni (~8.5 wt%). It is interesting to note that both bright and dark phases are Fe rich, which indicates the dissolution of Fe from the ferritic stainless steel base metal into the molten brazing filler metal during brazing. A further discussion on the microstructure of the interlayer is outside the scope of the present study. The microstructures of the interlayer of brazing joints of stainless steels with Ni-based filler metal have been discussed in the open literature.[5,6]

The thickness of the diffusion zone can be approximated by the distribution of major alloying elements across the interface between the interlayer and the base metal through the EDS line scan. As expected, the EDS line scan results of four different alloying elements (Fe, Cr, Ni, and Si) show that the concentrations of those elements gradually change within the diffusion zone for all the brazing joints (Fig. 5). In the present study, the concentration curve of Ni, which is the major alloying element of the filler metal, was used to measure the thickness of the diffusion zone (Fig. 6). The thickness of the diffusion zone was measured by measuring the distance from the last peak of the concentration curve of Ni prior to the rapid decrease to the point of average Ni intensity of the 436 ferritic stainless steel, as schematically marked in Fig. 6(a). The diffusion zone thicknesses were measured on both the top and bottom sides of the interlayer for each specimen. Note that some fluctuations in the concentration curve of Ni were found in the interlayer zone. This is attributed to the two different Ni rich (bright) and Ni poor (dark) phases

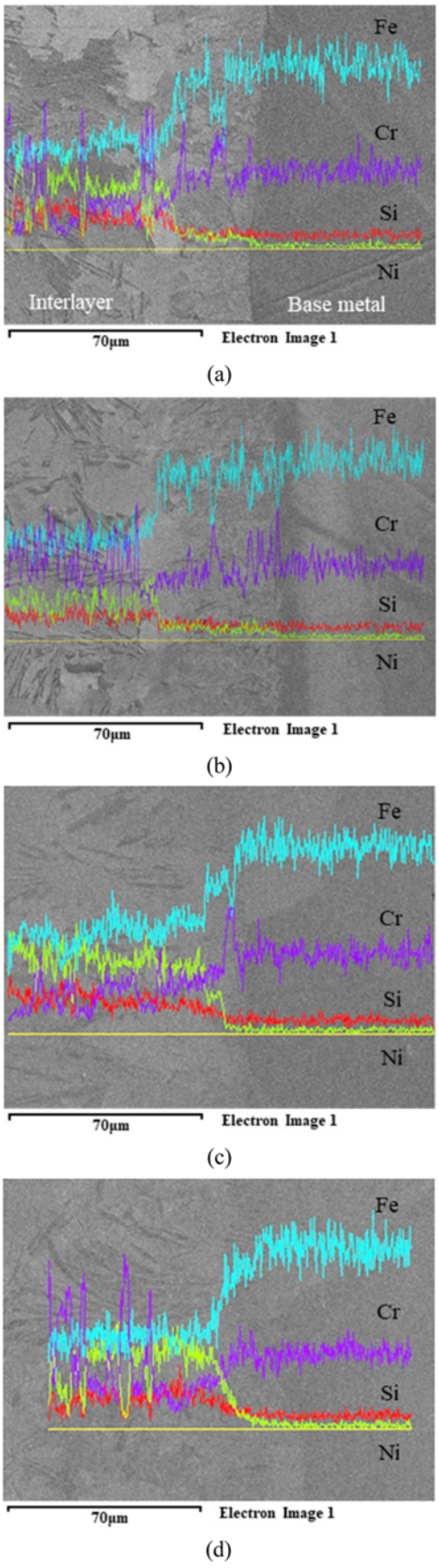

Fig. 5 SEM-EDS elemental line scans of Ni, Cr, Si, and Fe across the brazing joint: electrically assisted brazing for (a) t_h = 0 sec, (b) t_h = 5 sec and induction brazing for (c) t_h = 0 sec, and (d) t_h = 20 sec

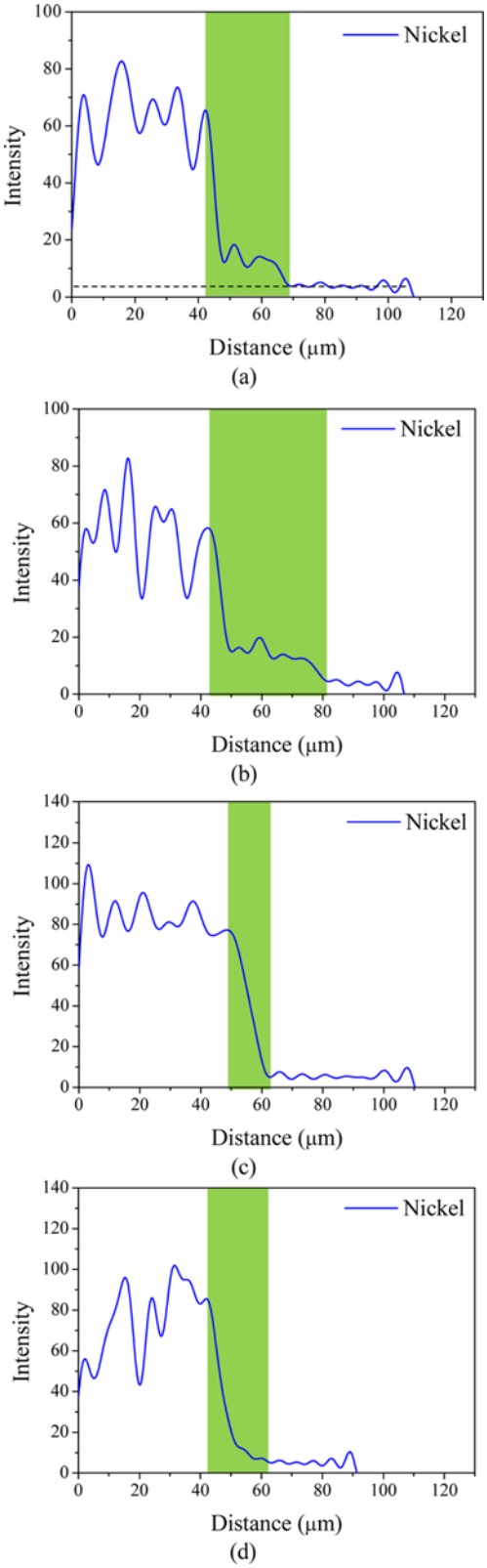

Fig. 6 The Ni distribution: electrically assisted brazing for (a) t_h = 0 sec, (b) t_h = 5 sec and induction brazing for (c) t_h = 0 sec, and (d) t_h = 20 sec

in the interlayer zone as marked in Fig. 4(c).

As expected,[7,21] measurements of the thickness of the diffusion zone show that the thickness increased as the holing time t_h increased (Table 3).

Table 3 The thickness of diffusion zone in brazing experiment with various brazing conditions

Type		Electrically assisted brazing for holding time (sec)			Induction brazing for holding time (sec)		
		$t_h = 0$ (or $t_D = 2$)	$t_h = 5$ (or $t_D = 6.6$)	$t_h = 10$ (or $t_D = 11.7$)	$t_h = 0$ (or $t_D = 9$)	$t_h = 10$ (or $t_D = 18.5$)	$t_h = 20$ (or $t_D = 28.3$)
Thickness of Ni gradient (μm)	Top 01	29.5	40.1	45.6	15.7	16.8	19.5
	Top 02	24.6	39.4	43.5	11.5	17.4	17.3
	Bottom 01	32.6	37.4	40.3	12.6	18.5	22.1
	Bottom 02	30.1	37.1	38.2	14.2	14.5	20.7
	Average	29.2	38.5	41.9	13.5	16.8	19.9

However, a comparison of the results for electrically assisted brazing and induction brazing shows that the thickness of the diffusion zone can vary significantly depending on the heat source. The diffusion zones of electrically assisted brazing joints appear to be much thicker than those of induction brazing joints. Even the diffusion zone for electrically assisted brazing with t_h = 0 sec is approximately 50% thicker than that for induction brazing with t_h = 20 sec. The significantly thicker diffusion zones of electrically assisted brazing joints suggest that the athermal effect of the electric current[9,11] occurred during electrically assisted brazing in addition to resistance heating. The result of induction brazing was not much different from that of furnace brazing with similar experimental parameters.

For induction brazing, the thickness of diffusion zone, X_D, in Table 3 can be simply related to the diffusivity and the diffusion time as[22]

$$X_D \propto \sqrt{Dt_D} \quad (1)$$

where D and t_D are the diffusivity of Ni to the ferritic stainless steel and the diffusion time, respectively. In the present study, the diffusion time is defined as the period in which the joint temperature is above the liquidus (1000°C) of the filler metal, as listed in Table 3. The thickness of the diffusion zone can be plotted as a function of the square root of diffusion time, $\sqrt{t_D}$, as shown in Fig. 7. As listed in Table 3, the figure shows that resistance heating using an electric current result in a significant offset in the thickness of the diffusion zone. Note that the slope of the linear least square fit (LSF) for the results of induction brazing can be easily correlated with diffusivity during induction brazing. However, one may not simply correlate the slope of the LSF from the electrically assisted brazing results with the diffusivity during electrically assisted brazing, since each result for the electrically assisted brazing has both a different diffusion time and a different history of electric current density. In general, the enhanced diffusion by electric current corresponds well with the enhanced diffusion of Zn/Cu couples by electric current.[10] However, it may be too early to explain the effect of electric current on diffusion by using the theory of electron migration, since a few recent studies reported experimental results that cannot be simply explained by the theory of electron migration.[11,17,23] Even though various hypotheses are being actively investigated,[24-26] the exact mechanism related with the athermal effect of electric current, has not been identified yet.

Fracture during tensile lap-shear tests occurred in the interlayer along the interface between the diffusion zone and the interlayer for all electrically assisted and induction brazing joints (Fig. 8). For both electrically assisted and induction brazing, the shear strength increased with increasing holding time t_h (or the brazing time t_D), as shown in

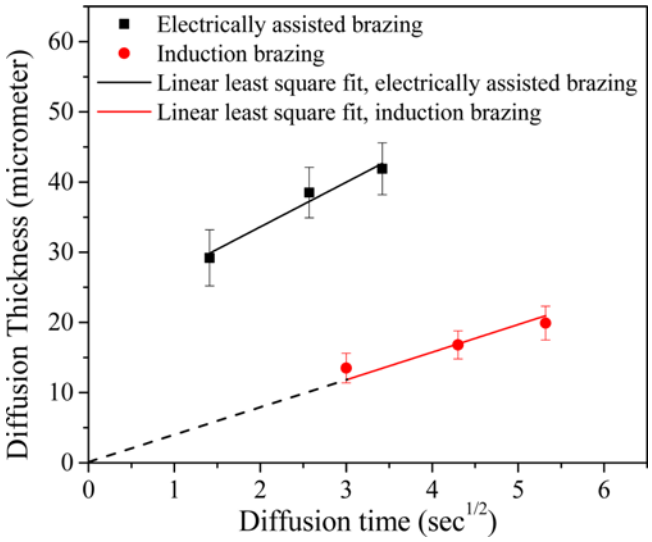

Fig. 7 The diffusion thickness as a function of the square root of diffusion time

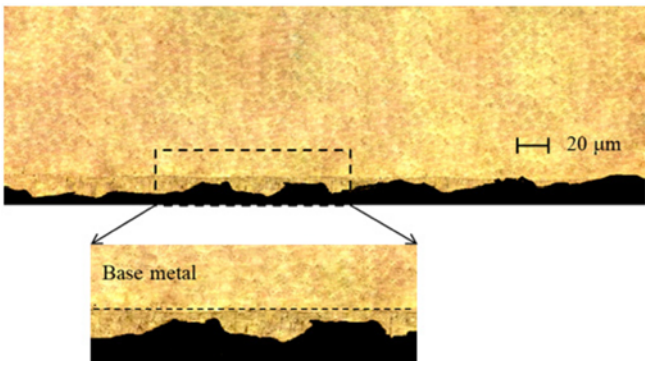

Fig. 8 Cross-sectional image of brazing joints after shear test for electrically assisted brazing specimen for t_h = 5 sec

Fig. 9. A comparison of the shear strength of the joints shows that electrically assisted brazing induced a higher fracture strength than induction brazing even with a shorter holding time or brazing time. For example, electrically assisted brazing with t_h = 0 sec (or t_D = 2 sec) induced an average fracture strength of 184 MPa, which is higher than the result of the induction brazing with t_h = 10 sec (or t_D = 18.5 sec) and comparable to the result of induction brazing with t_h = 20 sec (or t_D = 28.3 sec), as indicated in Fig. 9. The higher fracture strength obtained by electrically assisted brazing corresponds well with the

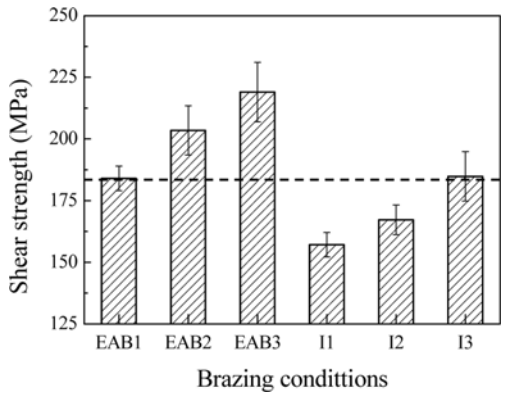

Fig. 9 Comparison of shear strength: electrically assisted brazing for t_h = 0 sec (EAB1), t_h = 5 sec (EAB2), and t_h = 10 sec (EAB3) and induction brazing for holding time of t_h = 0 sec (I1), t_h = 10 sec (I2), and t_h = 20 sec (I3)

higher diffusion of Ni into the base ferritic stainless steel in electrically assisted brazing, since the strength of the brazing joint is affected by the diffusion of main alloying elements in the filler metal to the base metal.[22,27]

4. Conclusions

In the present study, the effectiveness of electrically assisted brazing was compared with that of conventional induction brazing by joining ferritic stainless steel sheets with a Ni-based filler metal. As shown in the microstructural analysis results, the electric current during electrically assisted brazing significantly enhanced the diffusion between the filler metal and the ferritic stainless steel sheets in comparison with induction brazing. The enhanced diffusion during electrically assisted brazing strongly supports the athermal effect of electric current, which is closely related to the theory of electroplasticity. Also, the results of mechanical tests showed that electrically assisted brazing provided a joint strength comparable to the strength of the induction brazing joint with a significantly shorter processing time. Therefore, the electrically assisted brazing provides the technical advantage that the process time can be significantly reduced without sacrificing the joint strength (or a higher joint strength with a similar process time) in comparison with induction brazing. Also, due to the significantly higher heating rate, the energy loss to the environment during heating is likely to be less in electrically assisted brazing than in induction brazing. These superior properties of electrically assisted brazing over induction brazing could make electrically assisted brazing a strong candidate to replace conventional induction brazing.

ACKNOWLEDGEMENT

This research was supported by the National Research Foundation of Korea (NRF) grant funded by the Ministry of Science, ICT & Future Planning (MSIP) (No. NRF-2015R1A5A1037627). This research was supported by the Ministry of Trade, Industry & Energy (MOTIE), Korea Institute for Advancement of Technology (KIAT) through the Encouragement Program for The Industries of Economic Cooperation Region.

Conflict of Interest

On behalf of all authors, the corresponding author states that there is no conflict of interest.

REFERENCE

1. Mohandas, T., Reddy, G. M., and Naveed, M., "A Comparative Evaluation of Gas Tungsten and Shielded Metal Arc Weld of a Ferritic Stainless Steel," Journal of Materials Processing Technology, Vol. 94, Nos. 2-3, pp. 133-140, 1999.
2. Kim, K.-H., Bang, H.-S., Ro, C.-S., and Bang, H.-S., "Influence of Preheating Source on Mechanical Properties and Welding Residual Stress Characteristics in Ultra Thin Ferritic Stainless Steel Hybrid Friction Stir Welded Joints," International Journal of Precision Engineering and Manufacturing-Green Technology, Vol. 4, No. 4, pp. 393-400, 2017.
3. Taban, E., Deleu, E., Dhooge, A., and Kaluc, E., "Laser Welding of Modified 12% Cr Stainless Steel: Strength, Fatigue, Toughness, Microstructure and Corrosion Properties," Materials and Design, Vol. 30, No. 4, pp. 1193-1120, 2009.
4. Yang, R.-T. and Chen, Z.-W., "A Study on Fiber Laser Lap Welding of Thin Stainless Steel," International Journal of Precision Engineering and Manufacturing, Vol. 14, No. 2, pp. 207-214, 2013.
5. Shiue, R. K., Wu, S. K., and Hung, C. M., "Infrared Repair Brazing of 403 Stainless Steel with A Nickel-based Braze Alloy," Metallurgical and Materials Transactions: A, Vol. 33, No. 6, pp. 1765-1773, 2002.
6. Ou, C. L., Liaw, D. W., Du, Y. C., and Shiue, R. K., "Brazing of 422 Stainless Steel using the AWS Classification BNi-2 Braze Alloy," Journal of Materials Science, Vol. 41, No. 19, pp. 6353-6361, 2006.
7. Wu, X., Chandel, R. S., Pheow, S. H., and Li, H., "Brazing of Inconel X-750 to Stainless Steel 304 using Induction Process," Materials Science and Engineering: A, Vol. 288, No. 1, pp. 84-90, 2000.
8. Lugscheider, E. and Partz, K. D., "High Temperature Brazing of Stainless Steel with Nickel-base Filler Metals BNi-2, BNi-5 and BNi-7," Welding Journal, Vol. 62, No. 6, pp. 160-164, 1983.
9. Conrad, H., "Electroplasticity in Metals and Ceramics," Materials Science and Engineering: A, Vol. 287, No. 2, pp. 276-287, 2000.
10. Li, Y., Yang, Y., and Feng, X., "Influence of Electric Current on Kirkendall Diffusion of Zn/Cu Couples," Journal of Materials Science and Technology, Vol. 24, No. 3, pp. 410-414, 2008.

11. Kim, M.-J., Lee, K., Oh, K. H., Choi, I.-S., Yu, H.-H., et al., "Electric Current-Induced Annealing During Uniaxial Tension of Aluminum Alloy," Scripta Materialia, Vol. 75, pp. 58-61, 2014.
12. Kim. M.-S., Vinh, N. T., Yu, H.-H., Hong, S.-T., Lee, H.-W., et al., "Effect of Electric Current Density on the Mechanical Property of Advanced High Strength Steels under Quasi-Static Tensile Loads," International Journal of Precision Engineering and Manufacturing, Vol. 15, No. 6, pp. 1207-1213, 2014.
13. Nguyen-T., H.-D., Oh, H.-S., Hong, S.-T., Han, H. N., Cao, J., et al., "A Review of Electrically-Assisted Manufacturing," International Journal of Precision Engineering and Manufacturing-Green Technology, Vol. 2, No. 4, pp. 365-376, 2015.
14. Thien, N. T., Hong, S.-T., Kim, M.-J., Han, H. N., Yang, D.-H., et al., "Electrically Assisted Bake Hardening of Complex Phase Ultra-High Strength Steels," International Journal of Precision Engineering and Manufacturing, Vol. 17, No. 2, pp. 225-231, 2016.
15. Oh, H.-S., Cho, H.-R., Park, H., Hong, S.-T., Chun, D.-M., et al., "Study of Electrically-Assisted Indentation for Surface Texturing," International Journal of Precision Engineering and Manufacturing-Green Technology, Vol. 3, No. 2, pp. 161-165, 2016.
16. Xu, Z., Peng, L., and Lai, C., "Electrically Assisted Solid-State Pressure Welding Process of SS 316 Sheet Metals," Journal of Materials Processing Technology, Vol. 214, No. 11, pp. 2212-2219, 2014.
17. Kim, W., Yeom, K.-H., Thien, N. T., Hong, S.-T., Min, B.-K., et al., "Electrically Assisted Blanking using the Electroplasticity of Ultra-High Strength Metal Alloys," CIRP Annals–Manufacturing Technology, Vol. 63, No. 1, pp. 273-276, 2014.
18. Baranov, S. A., Staschenko, V. I., Sukhov, A. V., Troitskiy, O. A., and Tyapkin, A. V., "Electroplastic Metal Cutting," Russian Electrical Engineering, Vol. 82, No. 9, pp. 477-479, 2011.
19. Ng, M. K., Li, L., Fan, Z., Go, R. X., Smith III, E. F., et al., "Joining Sheet Metals by Electrically-Assisted Roll Bonding," CIRP Annals–Manufacturing Technology, Vol. 64, No. 1, pp. 273-276, 2015.
20. Davies, J. and Simpson, P., "Induction Heating Handbook," McGraw-Hill, 1979.
21. Yu, C.-C., Su, P.-C., Bai, S. J., and Chuang, T.-H., "Nickel-Tin Solid-Liquid Inter-Diffusion Bonding," International Journal of Precision Engineering and Manufacturing, Vol. 15, No. 1, pp. 143-147, 2014.
22. Atabaki, M. M., Wati, J. N., and Idris, J. "Transient Liquid Phase Diffusion Brazing of Stainless Steel 304," Welding Journal, Vol. 92, pp. 57, 2013.
23. Thien, N. T., Jeong, Y.-H., Hong, S.-T., Kim, M.-J., Han, H. N., et al., "Electrically Assisted Tensile Behavior of Complex Phase Ultra-High Strength Steel," International Journal of Precision Engineering and Manufacturing-Green Technology, Vol. 3, No. 4, pp. 325-333, 2016.
24. Kim, M.-J., Lee, M.-G., Hariharan, K., Hong, S.-T., Choi, I.-S., et al., "Electric Current-Assisted Deformation Behavior of Al-Mg-Si Alloy under Uniaxial Tension," International Journal of Plasticity, Vol. 94, pp. 148-170, 2017.
25. Park, J.-W., Jeong, H.-J., Jin, S.-W., Kim, M.-J., Lee, K., et al., "Effect of Electric Current on Recrystallization Kinetics in Interstitial Free Steel and AZ31 Magnesium Alloy," Materials Characterization, Vol. 133, pp. 70-76, 2017.
26. Molotskii, M. and Fleurov, V., "Magnetic Effects in Electroplasticity of Metals," Physical Review B, Vol. 52, No. 22, pp. 15829-15834, 1995.
27. Khorram, A. and Ghoreishi, M., "Comparative Study on Laser Brazing and Furnace Brazing of Inconel 718 Alloys with Silver Based Filler Metal," Optics & Laser Technology, Vol. 68, pp. 165-174, 2015.

Viet Tien Luu
Ph.D. candidate of School of Mechanical Engineering, University of Ulsan. His research interest is advanced metal joining and forming.
E-mail: tienvietluu@gmail.com

Thi Kieu Anh Dinh
Ph.D. candidate of School of Mechanical Engineering, University of Ulsan. Her research interest is advanced metal forming.
E-mail: dinhkieuanhbg@gmail.com

Hrishikesh Das
Postdoctoral researcher of School of Mechanical Engineering, University of Ulsan. His research interest is friction stir welding.
E-mail: hrishichem@gmail.com

Ju-Ri Kim
M.S. graduate of School of Mechanical Engineering, University of Ulsan. She currently works for Hyundai Rotem Company. Her research interest is solid state joining.
E-mail: jrkim20110@gmail.com

Sung-Tae Hong

Professor of School of Mechanical Engineering, University of Ulsan. His research interest is advanced metal forming and solid state joining.
E-mail: sthong@ulsan.ac.kr

Hyun-Min Sung

Associate research engineer in Materials & Production engineering Research Institute, LG electronics. His research interest is structural materials.
E-mail: hyunmin.sung@lge.com

Heung Nam Han

Professor in Department of Materials Science & Engineering, Seoul National University. His research interest is the mechanical behavior and microstructure for materials.
E-mail: hnhan@snu.ac.kr